Article

Investigation on an Improved Household Refrigerator for Energy Saving of Residential Buildings

Jingyu Cao [1], Qiliang Wang [2], Mingke Hu [3],*, Xiao Ren [1], Weixin Liu [1], Yuehong Su [3] and Gang Pei [1],*

[1] Department of Thermal Science and Energy Engineering, University of Science and Technology of China, Hefei 230027, China; jycao@ustc.edu.cn (J.C.); rx1008@mail.ustc.edu.cn (X.R.); liuwx@mail.ustc.edu.cn (W.L.)

[2] Department of Building Services Engineering, The Hong Kong Polytechnic University, Kowloon, Hong Kong, China; qiliang.wang@polyu.edu.hk

[3] Department of Architecture and Built Environment, University of Nottingham, University Park, Nottingham NG7 2RD, UK; Yuehong.Su@nottingham.ac.uk

* Correspondence: Mingke.Hu@nottingham.ac.uk (M.H.); peigang@ustc.edu.cn (G.P.)

check for
updates

Abstract: The efficiency improvement of household refrigerators is of significance to electricity consumption reduction of residential buildings. The cold loss recovery in household refrigerators is a promising development direction. In this study, a refrigerator improved by heat pipes is designed to reduce the cold loss at freezer walls to enhance the overall efficiency of the refrigerator. A complete steady-state mathematical model is built for characterizing its overall energy saving behaviors by introducing the real structural parameters of a Midea BCD-111 refrigerator and measured temperature boundary conditions. The performances of the improved refrigerator are investigated with typical operating states, variable ambient temperature, and heat pipe design. The simulative results indicate that the cold loss of the freezer of the improved refrigerator can be reduced by 8.3–16.5%, and the energy saving capability is relatively reliable. Results verify that the cold loss recovery of the improved refrigerator is feasible in various operating conditions.

Keywords: household refrigerator; energy saving; building; heat pipe; cold loss recovery

1. Introduction

Worldwide demands for living quality grow rapidly with social and economic development [1], which leads to a considerable increase in domestic appliances in buildings [2]. As a representative, the popularity of household refrigerators prevents the reduction of the world's energy demand and CO_2 emissions, and its energy consumption is accounting for more than a quarter of the global residential electricity demand [3]. Thus, promoting new and efficient technologies for the efficiency advance in household refrigerators is extremely urgent. Great efforts have been made to enhance the performances of the key components, such as the compressor [4], the condenser, and the evaporator [5], to optimize the refrigeration cycle [6], to modify internal and external structural design [7], and to improve the thermal insulated behaviors [8]. However, there still exists a balance between cost and performance in the research field of household refrigerators [9]. Recently, an increasing number of new technologies have been applied for breaking this chain. Cheng et al. designed a heat storage evaporator and cold storage condenser for a household refrigerator, and its energy saving ratio was 32% [10]. Clito et al. enhanced the heat dissipation of a household refrigerator. The surface temperature close to the compressor was reduced by 11 °C [11]. Liu et al. proposed to adopt a diffuser pipe to enhance the behavior of a normal refrigerator, which leads to a 3.36–4.09% reduction in power consumption [12]. Cao et al. conducted a preliminarily experimental study on a cool-storage refrigerator for the use of

peak load shifting [13]; the follow-up research focused on the temperature management enhancement of household refrigerator [14]. Söylemez et al. used a hybrid cooling system to reduce cooling times and improve temperature stability of a household refrigerator [15]. Fatouh et al. suggested utilizing a ternary hydrocarbon mixture for household refrigerators and analyzed its energy and exergy behaviors in details [16]. Certain achievements have been made by the above attempts; however, the potential of a household refrigerator in its cold loss recovery did not arouse enough attention [17].

In a conventional household refrigerator, the temperature of the freezer is much lower than that of the fresh food compartment, and the only evaporating temperature of its cooling cycle is determined by the former. If the wasted cold energy of the freezer can be partly reused by the fresh food compartment, the overall energy consuming amount of the refrigerator is reduced while no additional exergy loss is generated. In our last study, this basic ideal was performed by utilizing the efficient heat transfer capability of two-phase loop thermosyphons to separate cold loss from the interlayer of the isolation wall of the freezer to the fresh food compartment [18]. In comparison to increasing the wall thickness, there was no reduction in the usable space of freezer by adopting this novel cold loss reduction method, and the cost increment of the improved refrigerator was relatively low, since the main structure of two-phase loop thermosyphons is made by low-cost aluminum alloy. Preliminary numerical research on the cold loss reduction behaviors of the modified freezer walls was performed in fixed operating conditions of an imaginary refrigerator, and results proved the effectiveness of heat pipes in the energy saving of household refrigerators. However, the overall energy saving capability is unknown, and the accuracy of quantitative analysis is still insufficient. Derived research focused on radical structural change of a household refrigerator, which deviates from the original intention of saving energy through simple structural improvement [19]. In the current research, new structure design of the refrigerator with heat pipes is proposed, a complete steady-state mathematical model is built for characterizing its overall energy saving behaviors, the real structural parameters of the Midea BCD-111 refrigerator and measured temperature boundary conditions are adopted for performance analysis of the improved refrigerator, and the influences of heat pipe design are studied in depth.

2. Operating Principle

The improved refrigerator is designed based on a Midea refrigerator numbered BCD-111, as shown in Figure 1. Two symmetrical heat pipes are installed into the refrigerator for reusing the wasted cold energy of the freezer. More specifically, only topside and side freezer walls are changed, and eight aluminum heat pipes are used to transport part of their cold loss to the fresh food compartment, as is depicted in Figure 2. Aluminum plates are adopted to enhance the heat transfer at evaporating and condensing sections. The diameter of the heat pipe and the thickness of aluminum plates are preliminarily designed as 6 mm. The evaporating sections of the heat pipes are designed to offer a support plate for the fresh food compartment.

The refrigerator is improved by wasted cold energy recovery at the freezer. As is compared in Figure 1, the modified walls of the improved freezer have a shunted heat transfer process. As one part of heat comes from the fresh food compartment, the heat leakage from the ambinet is reduced. The heat transfer processes of original and modified topside freezer walls are compared in Figure 3 as an example. The heat pipes change the temperature distribution of the freezer wall. In comparison of the installation position of heat pipes, the local temperature (T'_{HP}) is raised to the temperature of the heat pipes (T_{HP}). Thus, the external heat flux (Q_{out}) decreases, whereas the internal heat flux (Q_{in}) increases. The heat flux difference between them (Q_{HP}) is acquired from the fresh food compartment using heat pipe. It should be emphasized that the heat transfer enhancement between the fresh food compartment and freezer (which could also be easily done by reducing its internal thermal isolation) is just a side effect, and the main purpose of adding heat pipes is to decrease the overall heat leakage of the improved refrigerator.
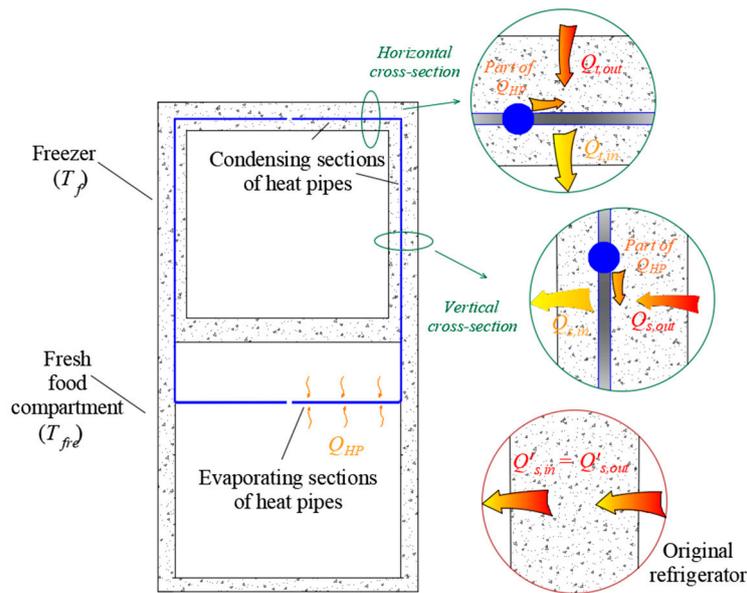
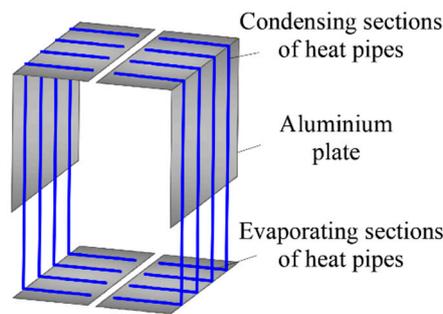**Figure 1.** Section views of the improved refrigerator.

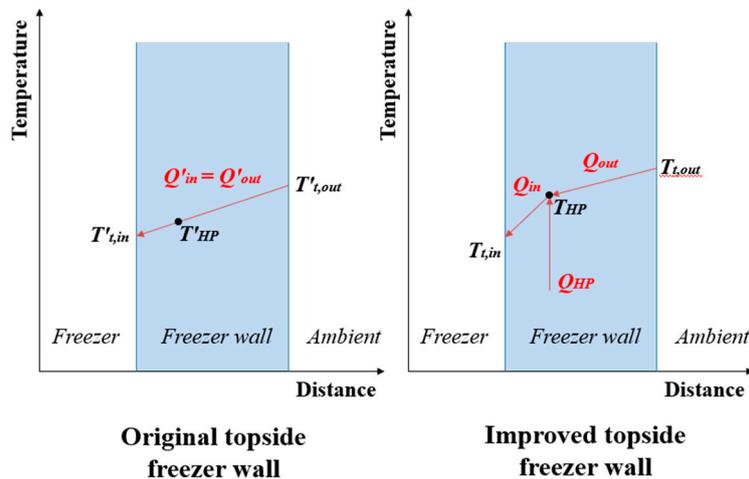**Figure 2.** Structural schematic of the heat pipes.

Figure 3. Heat transfer processes of original and modified topside freezer walls.

3. Measured Conditions of Midea BCD-111 Refrigerator

For performance comparison between the improved and the original refrigerators, the specific geometric parameters of Midea BCD-111 household refrigerator are measured. The length, the width, and the height of the freezer are 325 mm, 330 mm, and 300 mm, respectively, while the corresponding wall thicknesses are 80 mm, 70 mm, and 50 mm, respectively. The wall thickness between the freezer

and the fresh food compartment is 50 mm. The temperature boundary conditions are also tested at different operating states of the refrigerator, as shown in Table 1. The ambient temperature and the average air temperatures in the freezer (T_f) and the fresh food compartment (T_{fre}) are measured according to the National Standard GB/T 8059-2016. Since the temperatures at the outside surface of side walls of the BCD-111 refrigerator are related to its condensing temperature, the outside surface temperature of side freezer wall ($T_{s,out}$) is also measured. Detailed temperature measurement methods can be found in reference [19].

Table 1. Boundary conditions under different temperature gears and ambient temperatures [19].

Operating States of the Tested Refrigerator		T_f [°C]	T_{fre} [°C]	$T_{s,out}$ [°C]
Ambient Temperature [°C]	Temperature Gear			
25.0	C	−17.7	4.7	27.0
17.0	C	−16.0	5.2	18.1
20.0	C	−16.5	5.0	21.3
31.0	C	−20.2	2.9	32.6
25.0	A	−19.6	2.1	27.0
25.0	B	−19.3	2.6	27.0
25.0	D	−17.2	5.0	26.7

4. Mathematical Model

The simplified mathematical model is built for the original and the modified freezer of the BCD-111 refrigerator. The following hypotheses are adopted.

- The temperature fluctuation of air is neglected.
- The walls of refrigerator have the same heat conductive coefficient.
- Rectangular straight fin efficiency is adopted for aluminum plates [20].
- The heat transfer is steady-state and 1D.
- The temperatures at evaporating and condensing sections of heat pipes are considered uniform ($T_{HP} = T_{con} = T_{eva}$) since the internal two-phase thermal resistance is far less than the external convective thermal resistance.
- The external surface temperature of side freezer walls is given as a boundary condition due to the influence of condenser of the BCD-111 refrigerator.

The measured boundary conditions are utilized in following methods:

Boundary condition 1: the surrounding air temperatures are given for the original freezer walls (or the evaporating sections of heat pipes in fresh food compartment);
Boundary condition 2: the average outside wall temperatures are given for the improved freezer walls.

Based on the above hypotheses and boundary conditions, the thermal analyses of the original and improved refrigerator are conducted using iterative computations.

The heat fluxes at half of the topside freezer wall of the improved refrigerator are calculated based on the boundary condition 1, in which the heat conversion coefficient is calculated through self iteration:

$$Q_{t,out} = \frac{T_{amb} - T_{HP}}{\frac{1}{\alpha_{t,out}} + \frac{(\delta - X_{t,in})}{\lambda}} A_t \tag{1}$$

$$Q_{t,in} = \frac{T_{HP} - T_f}{\frac{1}{\alpha_{t,in}} + \frac{X_{t,in}}{\lambda}} A_t \tag{2}$$

where $Q_{t,out}$ and $Q_{t,in}$ are outside and inside heat fluxes, respectively; T_{amb}, T_{HP}, and T_f are ambient temperature, heat pipe temperature, and freezer temperature, respectively; $\alpha_{t,out}$ and $\alpha_{t,in}$ are the convective heat transfer coefficients of ambient and inside air, respectively; δ is the wall thickness; X_t is the ratio of wall thickness inside of heat pipes to the whole topside wall thickness; and A_t is the topside heat transfer area.

The heat fluxes at left or right freezer walls of the improved refrigerator are calculated based on the boundary condition 2.

$$Q_{s,out} = \frac{T_{s,out} - T_{HP}}{\frac{(\delta - X_{s,in})}{\lambda}} A_s \tag{3}$$

$$Q_{s,in} = \frac{T_{HP} - T_f}{\frac{1}{\alpha_{s,in}} + \frac{X_{s,in}}{\lambda}} A_s \tag{4}$$

where $Q_{s,out}$ and $Q_{s,in}$ are outside and inside heat fluxes, respectively; $T_{s,out}$ is the outside surface temperature of side freezer wall; $\alpha_{t,out}$ and $\alpha_{t,in}$ are the convective heat transfer coefficients of ambient and inside air, respectively; X_s is the ratio of wall thickness inside of heat pipes to the whole side wall thickness; and A_s is the side heat transfer area.

For the condensing section of heat pipes, the heat is released to the topside and the side freezer walls.

$$Q_{HP} = (Q_{s,in} + Q_{t,in}) - (Q_{s,out} + Q_{t,out}) \tag{5}$$

where Q_{HP} is the heat flux of heat pipes; $Q_{s,in}$ and $Q_{s,out}$ are inside and outside heat flux at each side freezer wall, respectively; and $Q_{t,in}$ and $Q_{t,out}$ are inside and outside heat flux at half of the topside freezer wall, respectively.

Meanwhile, the heat gain at the evaporating sections of heat pipes is as follows:

$$Q_{HP} = (\alpha_{eva,u} + \alpha_{eva,l})(T_{fre} - T_{HP})A_{eva} \tag{6}$$

where $\alpha_{eva,u}$ and $\alpha_{eva,l}$ are the convective heat transfer coefficients of upper and lower surfaces of the evaporating sections of heat pipes, respectively; T_{fre} is the fresh food compartment temperature; and A_{eva} is the area of the evaporating sections of heat pipes.

Based on the above calculations, the heat transfer state of the freezer of the improved refrigerator can be acquired by iterating T_{HP}. Besides, the heat fluxes at the front and the back freezer walls of the improved refrigerator or the freezer walls of the original refrigerator are easily calculated based on the boundary conditions 1 or 2, and thus the energy saving ratios of the freezer of the improved refrigerator are as follows.

$$\eta_{re,s} = (1 - \frac{C_s}{C_s'}) \times 100\% \tag{7}$$

$$\eta_{re,t} = (1 - \frac{C_t}{C_t'}) \times 100\% \tag{8}$$

$$\eta_{re} = (1 - \frac{C}{C'}) \times 100\% \tag{9}$$

where $\eta_{re,s}$, $\eta_{re,t}$, and η_{re} are the energy saving ratios of the side wall, the topside wall, and the whole freezer of the improved refrigerator, respectively; C, C_s, and C_t are freezer cold loss and cold losses at the side and the topside freezer walls for the improved refrigerator, respectively ($C_s = 2 \times Q_{s,out}$ and $C_t = 2 \times Q_{t,out}$); and C'_s, C'_t, and C' are the cold losses of the side wall, the topside wall, and the whole freezer of the original refrigerator, respectively.

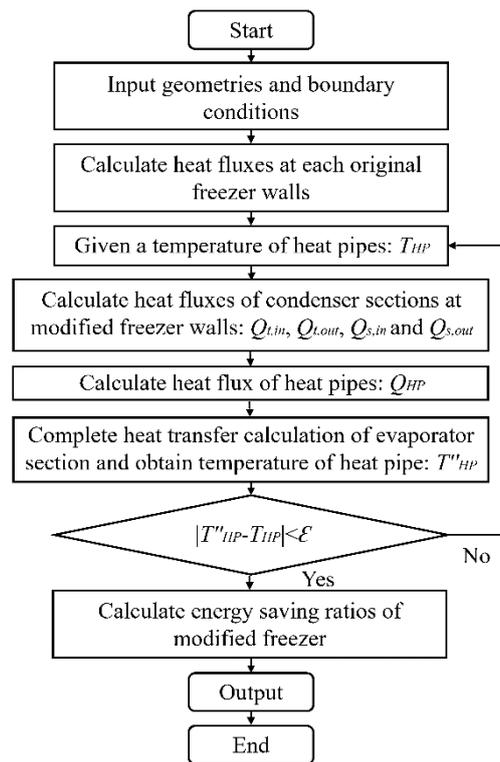The detailed calculation procedure is depicted in Figure 4.

Figure 4. Computation algorithm for the improved refrigerator.

5. Results and Discussion

5.1. Performances at Different Ambient Temperatures

Ambient temperature seriously affects the operating state of household refrigerators. When the temperature gear of the BCD-111 refrigerator is fixed to C, the temperature boundary conditions at ambient temperatures of 17.0 °C to 31.0 °C are adopted for analyzing the performances of the improved refrigerator. The common ratio of wall thickness inside of heat pipes to the whole wall thickness, X_{in} (namely $X_{in} = X_{t,in} = X_{s,in}$), is preliminarily set to 16%. The heat transfer area of the evaporating section of heat pipes (A_{eva}) is given as its maximum value of 0.146 m^2. In the side and the topside freezer walls of the improved refrigerator, considerable heat is transported to the freezer by heat pipes, which changes the thermal characteristics of the freezer walls. Since the outside surface temperature of side freezer walls is greatly affected by the ambient temperature, the side freezer walls of the original and the modified refrigerators are firstly compared in Figure 5. The convective heat transfer coefficients inside of the side freezer wall ($\alpha'_{s,in}$ and $\alpha_{s,in}$) both increase steadily with ambient temperature, but their difference gradually drops from 0.37 W·m^{-2}·K^{-1} to 0.22 W·m^{-2}·K^{-1} (the radiative heat flux is relatively low and thus is neglected to simplify the calculation). Correspondingly, the outside surface temperature of the original side freezer wall decreases from −11.5 °C to −13.8 °C, while that of the modified one reduces from −9.0 °C to −12.0 °C, and the gap between them gradually narrows from 2.5 °C to 1.8 °C. The above phenomena show that inside heat transfer of the modified side freezer wall is enhanced due to the existence of heat pipes, and the influence of heat pipes steadily decreases as the heat leakage increases with the ambient temperature.

This section is not mandatory, but may be added if there are patents resulting from the work reported in this manuscript.

Figure 6 further compares the cold loss recovery behaviors of the side and the topside freezer walls. When the ambient temperature is 20 °C, the cold loss at the inside surfaces of the two side modified freezer walls ($C_{s,in}$) is 5.0 W, and the corresponding outside one ($C_{s,out}$) is reduced to 2.4 W. Meanwhile, the cold loss at the inside surface of the topside modified freezer wall ($C_{t,in}$) is 2.2 W,

and the corresponding outside one ($C_{t,out}$) drops to 1.0 W. In comparison to the original freezer walls, about 24.7% of the cold loss of side freezer walls and 21.7% of the cold loss of topside freezer wall are recovered by the heat pipes. With a raising ambient temperature, $C_{s,out}$ increases from 2.1 W to 3.8 W, and $C_{t,out}$ enlarges from 0.9 W to 1.7 W. The cold loss reduction ratios of side and topside freezer walls ($\eta_{s,re}$ and $\eta_{t,re}$, respectively) significantly drops from 28.3% to 15.0% and from 25.3% to 12.8%, respectively. The cold loss recovery behavior of modified side freezer wall remains better than the topside one, and their cold loss recovery capabilities are both considerably restricted by a high ambient temperature.
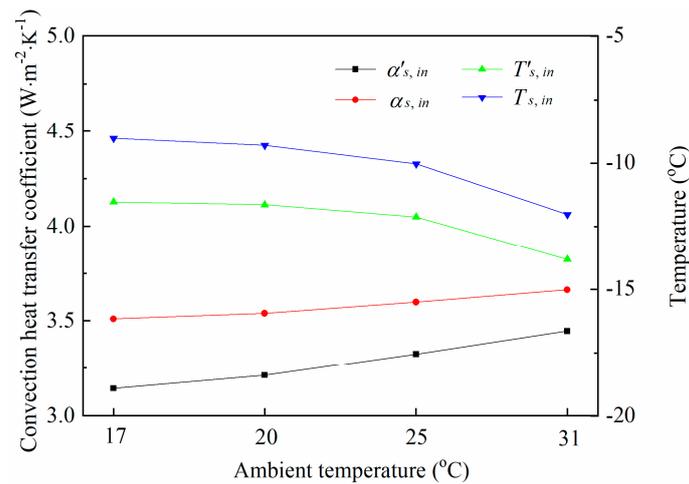
Figure 5. Inside heat transfer characteristics inside of the topside freezer wall at various ambient temperatures.
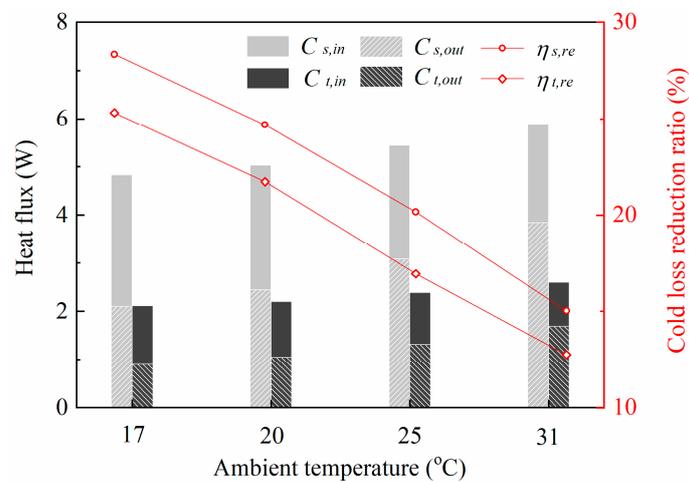
Figure 6. Cold loss comparison between side and topside freezer walls at various ambient temperatures.

The overall cold loss recovery performances of the modified freezer at various ambient temperatures are presented in Figure 7. The cold loss of original freezer increases from 6.4 W to 10.0 W, while that of the modified freezer raises from 5.3 W to 9.2 W with a raising ambient temperature. Correspondingly, the cold loss reduction ratio of the freezer (η_{re}) decreases from 16.5% to 8.3%. The results indicate that more cold loss could be recycled by the heat pipes when the refrigerator runs with a lower ambient temperature. In general, the energy saving of the improved refrigerator is reliable when ambient condition varies within a typical range.
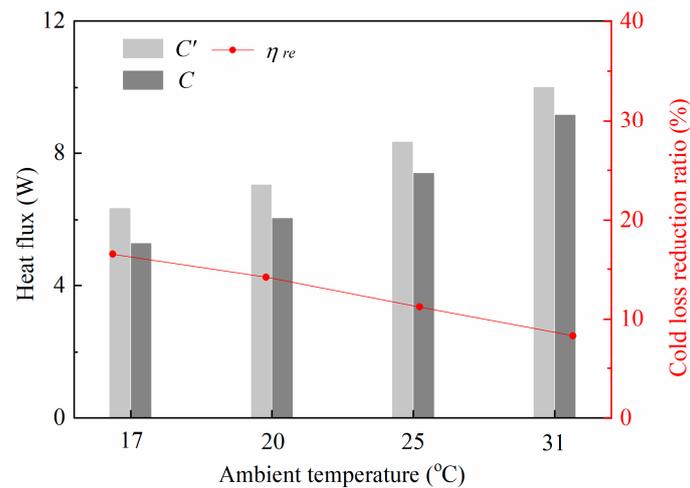
Figure 7. Cold loss recovery performances of modified freezer at various ambient temperatures.

5.2. Performances at Different Temperature Gears

When the ambient temperatures, A_{eva} and X_{in}, are fixed to 25.0 °C, 0.146 m^2, and 16%, respectively, and the temperature gears are given as A~D, the measured boundary conditions are utilized to further compare the performances of original and improved refrigerators. The representative heat transfer parameters of original and improved side freezer walls are shown in Figure 8. As the temperature gear is adjusted from A to D, the inside convective heat transfer coefficient for the original side wall ($\alpha'_{s,in}$) remains close to 3.34 W·m^{-2}·K^{-1}, whereas that for the modified one ($\alpha'_{s,in}$) remains at about 3.59 W·m^{-2}·K^{-1}. The inside surface temperature for the modified side wall ($T_{s,in}$) raises from −12.1 °C to −9.6 °C; and the inside surface temperature for the original side wall ($T'_{s,in}$) raises from −13.9 °C to −11.8 °C. When the temperature gear changes from A to D, $T_{s,in}$ remains higher than $T'_{s,in}$, and their difference slightly enlarges from 1.8 °C to 2.1 °C. The enhancement on the inside heat transfer of the modified side freezer wall intensifies as the inside temperatures of the refrigerator raise.
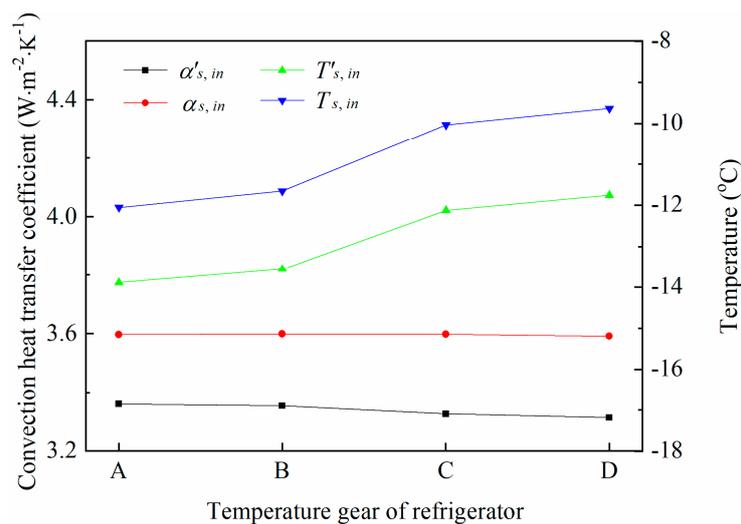

Figure 8. Inside heat transfer characteristics of the topside freezer wall at various temperature gears.

The topside freezer wall of the improved refrigerator is with boundary condition 1, and thus the bilateral heat transfer characteristics are affected by the heat pipe. Figure 9 shows the surface temperature comparison between the original and the modified topside freezer walls under different temperature gears. Take temperature gear B for example, the outside surface temperature increases from 20.2 °C to 20.8 °C after adding the heat pipe, and the inside surface temperature correspondingly

increases from −11.6 °C to −9.9 °C. The existence of the heat pipes changes the temperature distribution in the topside freezer wall and reduces the temperature gap between its outside surface and ambient air. The phenomenon indicates that a considerable heat energy is transported from the fresh food compartment and flow into the freezer along with the outside heat leakage. Besides, the inside surface temperature for the modified topside freezer wall ($T_{t,in}$) raises from −10.3 °C to −7.9 °C, and the outside surface temperature for the original topside freezer wall ($T'_{t,out}$) slightly increases from 19.4 °C to 20.3 °C. The inside surface temperature for the original topside freezer wall ($T'_{t,in}$) and the outside surface temperature for the modified topside freezer wall ($T_{t,out}$) remain close to −11.5 °C and 20.8 °C, respectively. Results confirm that the influence of heat pipes intensifies as the inside temperatures of the refrigerator raise.
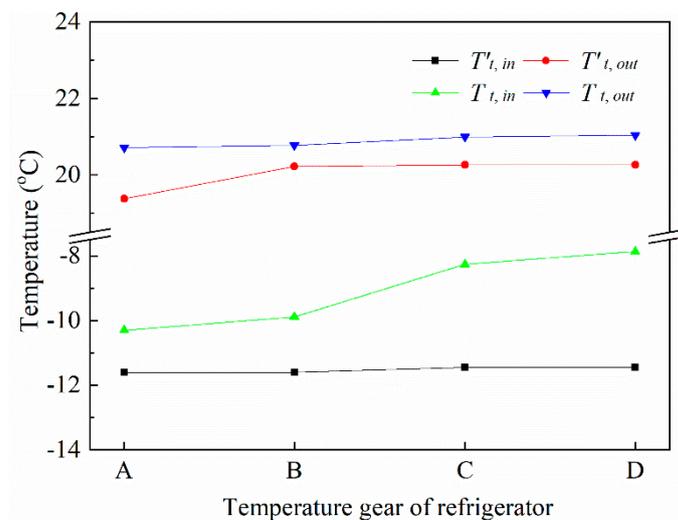

Figure 9. Surface temperatures of the side freezer wall versus temperature gear.

The heat transfer behaviors of the heat pipes are further studied to support the above analyses. As shown in Figure 10, the temperature of the heat pipes (T_{HP}) raises from −2.8 °C to −0.4 °C as the temperature gear is varied from A to D, and the difference between the air temperature at the fresh food compartment and T_{HP} enlarges from 4.9 °C to 5.4 °C. Correspondingly, the heat transfer capability of heat pipes enhances and its heat flux (Q_{HP}) increases from 3.0 W to 3.5 W. Heat pipes provide a cold loss recovery function for the freezer, and the heat shunt amount is closely affected by the temperature gear of the refrigerator. Since the temperature of evaporating sections of heat pipes in the fresh food compartment is close to 0 °C and is much higher than the temperature of the original evaporator of the refrigerator, the problem of frosting in the evaporating sections of the heat pipes is less serious.

Figure 11 compares the cold losses of the original and the modified freezer to overall evaluate the cold loss recovery behaviors of the improved refrigerator. Taking temperature gear B as an example, the cold loss of the freezer drops 0.9 W after adding heat pipes, which means 10.1% of cold loss can be recovered by the heat pipe. When the temperature gear varies from A to D, the cold losses of the original and the modified freezers both decrease 0.6 W, and the cold loss reduction ratio (η_{re}) correspondingly increases from 9.7% to 11.6%. On the whole, the improved refrigerator can effectively reduce the cold loss of the freezer even if the temperature gear of the refrigerator changes. The energy saving performance slightly enhances as the cold loss amount decreases with increasing inside temperatures of the refrigerator.
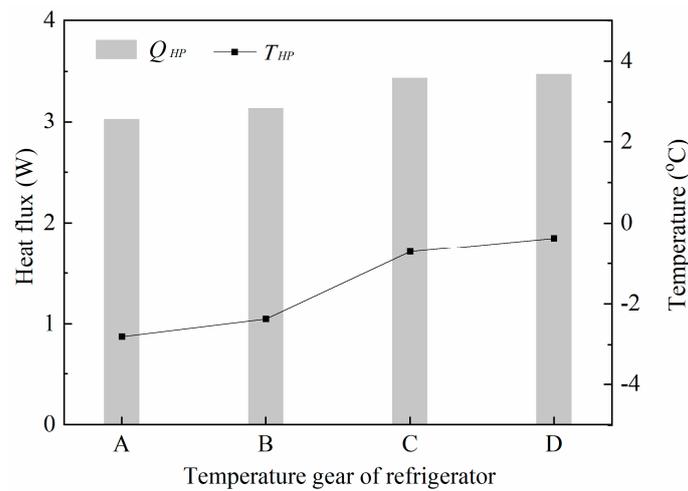
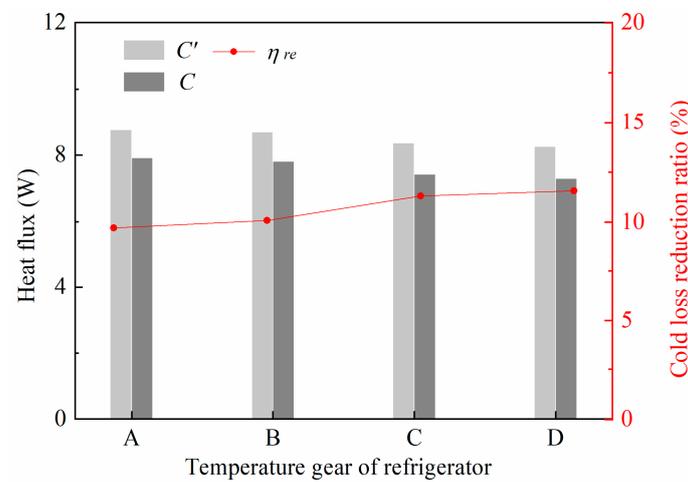**Figure 10.** Heat flux and temperature of heat pipes versus temperature gear.

Figure 11. Cold loss recovery behaviors of the improved refrigerator for different temperature gears.

5.3. Performances at Different Heat Pipe Design

In the above calculations, the heat transfer area of the evaporating sections of heat pipes is fixed, and its specific location in the side and the topside freezer wall is also set to the same. In this section, the heat transfer area of the evaporating sections of heat pipes along with the distances between the condensing sections of heat pipes and the inner walls are changed to further evaluate the influences of the heat pipe design. The behaviors of the improved refrigerator are analyzed for ambient temperature of 25 °C and temperature gear C.

The heat transfer area of the evaporating sections of heat pipes (A_{eva}) is firstly reduced from 0.146 m^2 to 0.094 m^2, while the ratio of length to width remains constant. The variations of the average convective heat transfer coefficients of the upper and the lower surfaces of the evaporating sections of heat pipes (α_{eva}) and the temperature of the heat pipes (T_{HP}) are shown in Figure 12. As the heat transfer area reduces 9.8%, 19.0%, 27.8%, and 36.0%, α_{eva} raises gradually from 2.68 W·m^{-2}·K^{-1} to 2.83 W·m^{-2}·K^{-1}, 2.78 W·m^{-2}·K^{-1}, 2.73 W·m^{-2}·K^{-1}, and 2.89 W·m^{-2}·K^{-1}, respectively. Correspondingly, T_{HP} decreases from −0.7 °C to −0.9 °C, −1.2 °C, −1.4 °C, and −1.7 °C, respectively. The convective heat transfer capability of the evaporating sections of heat pipes per unit area gradually increases as the temperature gap between the heat pipes and the fresh food compartment enlarges. The heat transfer area of the evaporating sections of heat pipes could considerably affect the internal heat transfer of the improved refrigerator.
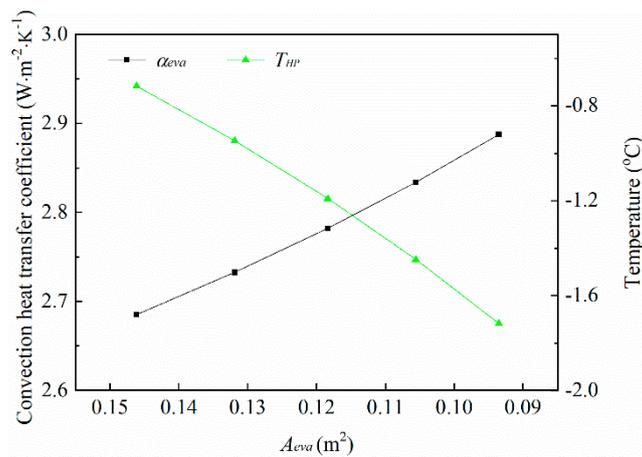
Figure 12. Heat transfer characteristics of the heat pipes at A_{eva}.

The impact of heat transfer area reduction of the evaporating sections of heat pipes on the overall behaviors of the improved refrigerator are further shown in Figure 13. When A_{eva} reduces from 0.146 m^2 to 0.094 m^2, the heat flux of the heat pipes (Q_{HP}) drops from 3.4 W to 2.8 W, and the heat flux decreasing ratio is about 80.4%. Correspondingly, the cold loss reduction ratio (η_{re}) decreases from 11.2% to 9.3%, and its decreasing ratio is about 82.8%. Results indicate that reduction on the heat transfer area of heat pipes in the fresh food compartment weakens the heat transfer of the heat pipes and thus causes a performance degradation of the improved refrigerator. However, the simulation also proves that a slight sacrifice of heat transfer area for the convenience of design and manufacture of the improved refrigerator is feasible.
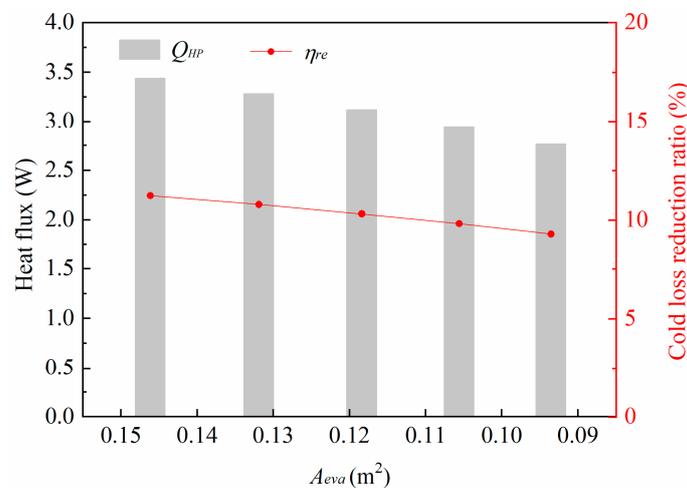

Figure 13. Behaviors of improved refrigerator versus at various A_{eva}.

Thereafter, given the maximum A_{eva} of 0.146 m^2, the common ratio of wall thickness inside of heat pipes to the whole wall thickness (X_{in}) is changed from 10% to 25%, and the temperatures of heat pipes and cold reduction ratios of side and topside freezer walls are shown in Figure 14. The temperature of heat pipes (T_{HP}) raises from −2.1 °C to 1.0 °C with increasing X_{in}. Correspondingly, the cold loss reduction ratio of the side freezer wall ($\eta_{s,re}$) and that of the topside freezer wall ($\eta_{t,re}$) gradually decrease from 20.7% to 18.1% and from 18.6% to 12.7%, respectively. Given the same location of the heat pipe, the cold loss reduction capability of the modified side freezer wall remains higher than that of the topside one, but the gap between $\eta_{s,re}$ and $\eta_{t,re}$ significantly enlarges from 2.1% to 5.4%. The temperature of heat pipes is closely related with its installation position in the freezer walls, and the cold loss reduction behavior of the side freezer walls is relatively more stable, even if the location

of heat pipes changes. Correspondingly, Figure 15 shows the overall behaviors of the modified freezer with increasing X_{in}. Cold loss of the modified freezer (C) slightly drops from 7.3 W to 7.6 W, and cold loss reduction ratio (η_{re}) decreases from 12.1% to 8.9% as X_{in} increases from 10% to 25%. The overall cold loss recovery amounts of heat pipes at various installation positions remain relatively stable. These results certify the reliability of the energy saving function of the improved refrigerator.
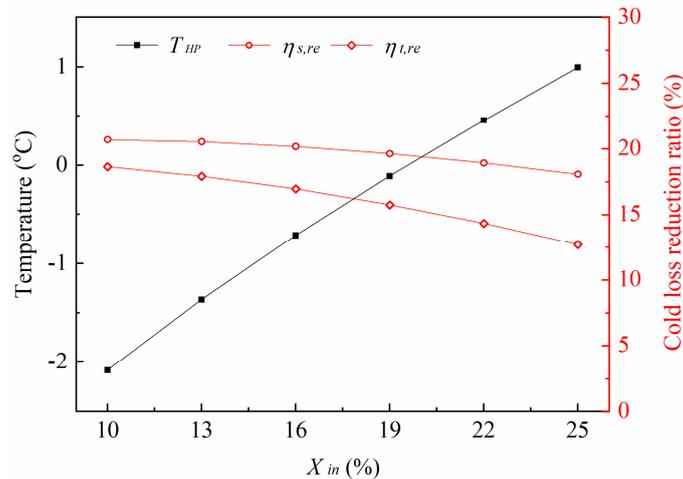
Figure 14. Temperatures of heat pipes and cold reduction ratios of side and topside freezer walls at various X_{in}.
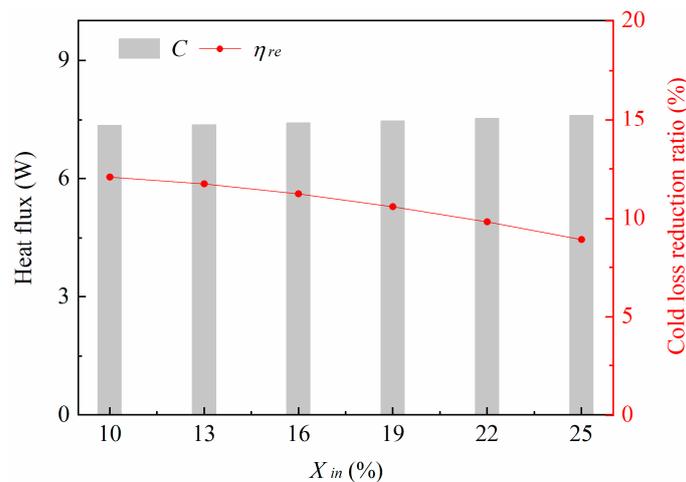

Figure 15. Overall cold loss of the modified freezer and cold loss reduction ratio versus X_{in}.

Furthermore, the locations of the condensing sections of heat pipes in the side and the topside freezer walls are individually varied, and the behaviors of the improved refrigerator are evaluated to reveal the energy saving difference at the side and the topside freezer walls. The ratio of wall thickness inside of heat pipes to the whole side wall thickness ($X_{s,in}$) is varied from 10% to 25%, while that for topside freezer wall ($X_{t,in}$) is fixed to 16%, and the calculated results are shown in Figure 16. T_{HP} raises from −1.8 °C to 0.5 °C, η_{re} decreases from 11.7% to 9.4%, and their variation ranges are smaller compared with the operating states with changing $X_{s,in}$ and $X_{t,in}$ together (shown in Figures 14 and 15). In particular, $\eta_{s,re}$ drops from 19.4% to 11.1% whereas $\eta_{t,re}$ raises from 16.8% to 24.0%. The temperature distribution at the topside freezer wall is affected by the raising T_{HP}, and thus its cold loss drops, even if $X_{t,in}$ is constant. For comparison, the behavior of the improved refrigerator is shown in Figure 17 as $X_{t,in}$ is varied from 10% to 25% with a fixed $X_{s,in}$. Correspondingly, $\eta_{s,re}$ increases from 16.0% to 18.2%, $\eta_{t,re}$ reduces from 23.7% to 13.6%, T_{HP} slightly raises from −1.0 °C to −0.3 °C, and η_{re} decreases from 11.5% to 10.5%. The performance responses to the variation of $X_{t,in}$ are much weaker than those of

$X_{s,in}$, which indicates the location of condensing sections of heat pipes at the topside freezer wall plays a more important role. Generally, properly adjusting the location of condensing sections of heat pipes at each freezer can vary the cold loss recovery capability of the improved refrigerator, and the energy saving design is feasible as $X_{s,in}$ and $X_{t,in}$ are changed between 10% to 25%.
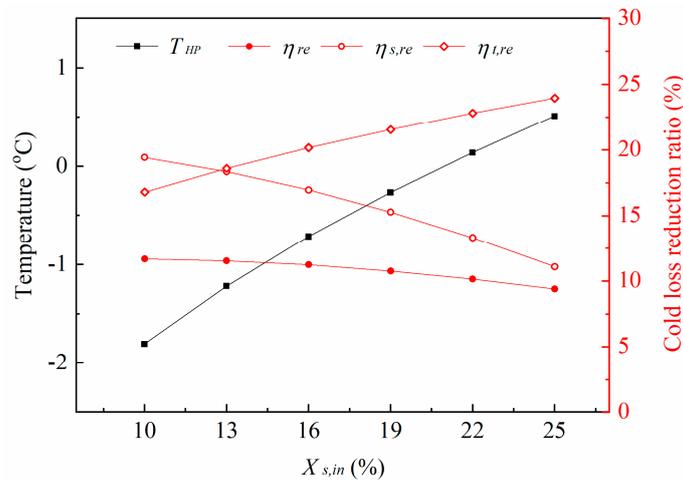

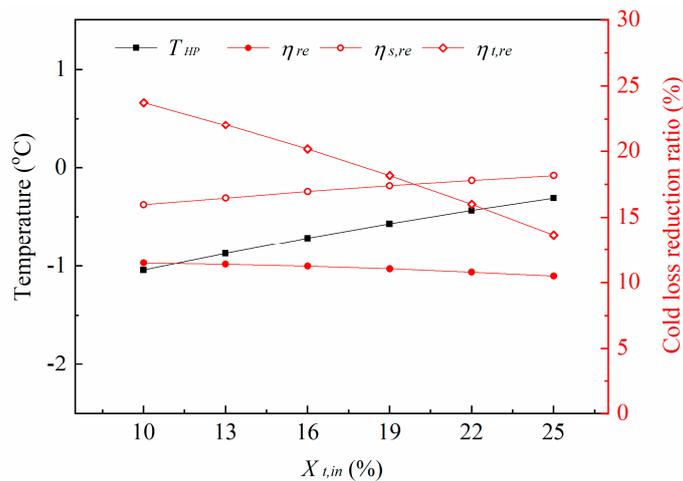**Figure 16.** Behaviors of improved refrigerator versus $X_{s,in}$ when $X_{t,in}$ is 16%.

Figure 17. Behaviors of improved refrigerator versus $X_{t,in}$ when $X_{s,in}$ is 16%.

6. Conclusions

An improved household refrigerator with heat pipes was designed to reduce the energy consumption of residential buildings. A simplified mathematical model was built combining the structure parameters and measured temperature boundary conditions of the BCD-111 refrigerator. The energy-saving performance of this improved refrigerator was numerically investigated by changing the temperature gear of the refrigerator from A to D, raising the ambient temperature from 17 °C to 31 °C, and varying the specific design of the heat pipes. The cold loss reduction ratios of the modified freezer were 8.3–16.5%, 9.7–11.6%, 9.3–11.2% and 8.9–12.1%, respectively, as responses to changing ambient temperature, temperature gear, heat transfer area, and location of heat pipes. Since the additional aluminum heat pipes and plates in the improved refrigerator have a relatively low cost, long service life, and little maintenance requirement, reusing wasted cold energy of a freezer is a feasible improvement method for a traditional household refrigerator. The current problem may be that the manufacturing processes of the improved refrigerator are more complex, and further research is required to reduce its manufacturing difficulty.

Nomenclature

A	heat transfer area [m^2]
amb	ambient air
C	cold loss [W]
HP	heat pipes
Q	heat flux [W]
R	thermal resistance [K·W^{-1}]
T	temperature [°C]
X_{in}	ratio of wall thickness inside of heat pipes to whole wall thickness [%]

Greek letters

α	convective heat transfer coefficient [W·m^{-2}·K^{-1}]
δ	wall thickness [m]
ε	iteration error
λ	heat conductivity coefficient [W·m^{-1}·K^{-1}]
η	ratio [%]

Superscripts

$'$	original refrigerator
$''$	iterative value

Subscripts

1	boundary condition 1
2	boundary condition 2
con	condensing section
HP	heat pipe
d	heat conduction
eva	evaporating section
f	freezer
fre	fresh food compartment
in	inside
our	outside
re	recovery
s	side freezer wall
t	topside freezer wall
v	convective heat transfer
w	freezer wall

References

1. Zhao, H.X.; Magoules, F. A review on the prediction of building energy consumption. *Renew. Sustain. Energy Rev.* **2012**, *16*, 3586–3592. [CrossRef]
2. Jones, R.V.; Fuertes, A.; Lomas, K.J. The socio-economic, dwelling and appliance related factors affecting electricity consumption in domestic buildings. *Renew. Sustain. Energy Rev.* **2015**, *43*, 901–917. [CrossRef]
3. Pirvaram, A.; Sadrameli, S.M.; Abdolmaleki, L. Energy management of a household refrigerator using eutectic environmental friendly PCMs in a cascaded condition. *Energy* **2019**, *181*, 321–330. [CrossRef]
4. Jomde, A.; Bhojwani, V.; Deshnnukh, S. Challenges in implementation of a moving coil linear compressor in a household refrigerator. *Int. J. Ambient Energy* **2019**, 1–4. [CrossRef]

5.   Tosun, M.; Dogan, B.; Ozturk, M.M.; Erbay, L.B. Integration of a mini-channel condenser into a household refrigerator with regard to accurate capillary tube length and refrigerant amount. *Int. J. Refrig.* **2019**, *98*, 428–435. [CrossRef]

6.   Alhamid, M.; Nasruddin, N.; Susanto, E.; Vickary, T.; Budiyanto, M.A.J.E. Refrigeration Cycle Exergy-Based Analysis of Hydrocarbon (R600a) Refrigerant for Optimization of Household Refrigerator. *Evergreen* **2019**, *6*, 71–77. [CrossRef]

7.   Maiorino, A.; Del Duca, M.G.; Mota-Babiloni, A.; Greco, A.; Aprea, C. The thermal performances of a refrigerator incorporating a phase change material. *Int. J. Refrig.* **2019**, *100*, 255–264. [CrossRef]

8.   Kojima, K.; Shinagawa, E.; Uematsu, I.; Hayamizu, N.; Ooshiro, K. Vacuum Insulation Panel, Core Material, and Refrigerator. U.S. Patent Application 15/556,920, 22 August 2019.

9.   Kim, H.C.; Keoleian, G.A.; Horie, Y.A. Optimal household refrigerator replacement policy for life cycle energy, greenhouse gas emissions, and cost. *Energy Policy* **2006**, *34*, 2310–2323. [CrossRef]

10.   Cheng, W.L.; Ding, M.; Yuan, X.D.; Han, B.C. Analysis of energy saving performance for household refrigerator with thermal storage of condenser and evaporator. *Energy Convers. Manag.* **2017**, *132*, 180–188. [CrossRef]

11.   Afonso, C.F. Household refrigerators: Forced air ventilation in the compressor and its positive environmental impact. *Int. J. Refrig.* **2013**, *36*, 904–912. [CrossRef]

12.   Liu, Y.C.; Chen, K.; Xin, T.L.; Cao, L.H.; Chen, S.M.; Chen, L.X.; Ma, W.W. Experimental study on household refrigerator with diffuser pipe. *Appl. Therm. Eng.* **2011**, *31*, 1468–1473. [CrossRef]

13.   Cao, J.Y.; Li, J.; Zhao, P.H.; Jiao, D.S.; Li, P.C.; Hu, M.K.; Pei, G. Performance evaluation of controllable separate heat pipes. *Appl. Therm. Eng.* **2016**, *100*, 518–527. [CrossRef]

14.   Cao, J.Y.; Pei, G.; Chen, C.X.; Jiao, D.S.; Jing, L. Preliminary study on variable conductance loop thermosyphons. *Energy Convers. Manag.* **2017**, *147*, 66–74. [CrossRef]

15.   Soylemez, E.; Alpman, E.; Onat, A. Experimental analysis of hybrid household refrigerators including thermoelectric and vapour compression cooling systems. *Int. J. Refrig.* **2018**, *95*, 93–107. [CrossRef]

16.   Fatouh, M.; Abou-Ziyan, H.J.A.T.E. Energy and exergy analysis of a household refrigerator using a ternary hydrocarbon mixture in tropical environment–Effects of refrigerant charge and capillary length. *Appl. Therm. Eng.* **2018**, *145*, 14–26. [CrossRef]

17.   Moayednia, N.; Ehsani, M.R.; Emamdjomeh, Z.; Asadi, M.M.; Mizani, M.; Mazaheri, A.F.J.A.J.o.B.; Sciences, A. The effect of sodium alginate concentrations on viability of immobilized Lactobacillus acidophilus in fruit alginate coating during refrigerator storage. *Aust. J. Basic Appl. Sci.* **2009**, *3*, 3213–3226.

18.   Cao, J.Y.; Chen, C.X.; Gao, G.T.; Yang, H.L.; Su, Y.H.; Bottarelli, M.; Cannistraro, M.; Pei, G. Preliminary evaluation of the energy-saving behavior of a novel household refrigerator. *J. Renew. Sustain. Energy* **2019**, *11*, 015102. [CrossRef]

19.   Cao, J.Y.; Chen, C.X.; Hu, M.K.; Wang, Q.L.; Cannistraro, M.; Leung, M.K.H.; Pei, G. Numerical analysis of a novel household refrigerator with controllable loop thermosyphons. *Int. J. Refrig.* **2019**, *104*, 134–143. [CrossRef]

20.   Bergman, T.L.; Incropera, F.P.; DeWitt, D.P.; Lavine, A.S. *Fundamentals of Heat and Mass Transfer*; John Wiley & Sons: Hoboken, NJ, USA, 2011.